arXiv:1404.2763v2 [cond-mat.mes-hall] 17 Jul 2014

Effects of Screening on Propagation of Graphene Surface Plasmons

Ken-ichi Sasaki* and Norio Kumada
NTT Basic Research Laboratories, NTT Corporation,
3-1 Morinosato Wakamiya, Atsugi, Kanagawa 243-0198, Japan
(Dated: July 18, 2014)

Electromagnetic fields bound tightly to charge carriers in a two-dimensional sheet, namely surface plasmons, are shielded by metallic plates that are a part of a device. It is shown that for epitaxial graphenes, the propagation velocity of surface plasmons is suppressed significantly through a partial screening of the electron charge by the interface states. On the basis of analytical calculations of the electron lifetime determined by the screened Coulomb interaction, we show that the screening effect gives results in agreement with those of a recent experiment.

Plasmons, which consist of carriers and electromagnetic fields, are the principal elements of excited states in solids.[1] When carriers are confined in a two-dimensional layer, surface plasmons can exist. The electromagnetic fields appear outside the layer and can be sensitive to the screening effect provided, for example, by a metallic plate that is a part of a device,[2] which is not so obvious for other excited states in solids, such as electrons and phonons. A device composed of a two-dimensional sheet of carbons, graphene,[3,4] provides a great opportunity to study this sensitivity of surface plasmons, as was demonstrated by a recent time-resolved experiment, which we review below.

Figure 1(a) is the schematic of a transport experiment performed by Kumada *et al* on graphene grown by SiC sublimation.[5] After applying a current pulse with a frequency of a few GHz at the injection gate on epitaxial graphene, they observed the current induced at the detection gate located approximately 220 μm from the injection gate. Figure 1(b) shows an example of the current observed as a function of time. The waveform has a peak structure at 1.5 ns, which enabled the authors to define the propagation velocity of a pulse as the propagation distance divided by the peak time, i.e., $220\mu m/1.5\text{ns} \simeq 15\times10^4$ m/s. The details of a waveform, such as peak time, depend on the Fermi energy position E_F, which was controlled using a metal top gate in their experiment. As a result, they were able to find the E_F dependence of the velocity shown by the solid curve in Fig. 1(c). The velocity decreases as the Fermi energy approaches the Dirac point $E_F = 0$ eV. For a wide range of E_F the velocity is one order of magnitude smaller than the electron Fermi velocity $v_F \simeq 10^6$ m/s. Such a slow charge propagation in a gated graphene on SiC has been observed also for edge magnetoplasmons.[6] The velocity in a device without a top gate was observed to be one or two order of magnitude larger than v_F, suggesting that the presence/absence of the gate strongly affects the plasmon transport.

In this paper we provide a theoretical basis that is useful for studying the propagation velocity of surface plasmons in graphene, while paying particular attention to the effect of a metal gate on the transport properties.[29] We will show that in the absence of a metal gate, plasmons propagate faster than the electrons. In the presence of a metal gate, the propagation velocity is much slower than v_F when the screening effect provided by interface states is taken into account. Furthermore, slow-moving surface plasmons undergo a strong diffusion when E_F is near the Dirac point, which explains the drop at $E_F \simeq 0.1$ eV seen in Fig. 1(c).

We begin by showing that the group velocity of plasmons in graphene without a metal gate cannot be lower than $v_F/2$. The plasmon dispersion is derived from the zero value of the real part of the dielectric constant

$$\varepsilon_{E_F}(q,\omega) = 1 - v_q \mathrm{Re}\Pi_{E_F}(q,\omega) = 0, \tag{1}$$

where v_q is the Coulomb potential.[1,8,9] In the absence of a metal top gate, $v_q = 2\pi e^2/\varepsilon q$, where ε is the permittivity of a surrounding medium, q is the wavevector magnitude, and e is electron charge magnitude in vacuum ($e^2 = 1.44$ eV·nm). $\Pi_{E_F}(q,\omega)$ is the polarization function, which is a function of q, frequency ω, and E_F. Although the polarization function for doped graphene has been calculated in several papers,[8–10] we show it in Appendix A for clarity. Since $v_q > 0$, the solution of Eq. (1) exists only when $\mathrm{Re}\Pi_{E_F}(q,\omega) > 0$ is satisfied. It can be shown that $\mathrm{Re}\Pi_{E_F}(q,\omega) > 0$ when $\omega > v_F q$ and $\mathrm{Re}\Pi_{E_F}(q,\omega) < 0$ when $\omega < v_F q$, so that plasmons exist only when $\omega > v_F q$.[30] In the literature, $\omega < v_F q$ is referred to as an electron-hole continuum or an intraband single-particle excitation (or $\mathrm{SPE_{intra}}$) region, where plasmons do not exist. When $\omega > v_F q$, $\mathrm{Re}\Pi_{E_F}(q,\omega)$ is approximated in the $q \to 0$ limit by

$$\mathrm{Re}\Pi_{E_F}(q,\omega) \simeq \frac{|E_F|}{\pi}\left(\frac{q}{\hbar\omega}\right)^2. \tag{2}$$

On combining Eq. (1) with Eq. (2), we obtain the plasmon frequency[8,9]

$$\omega_{pl}(q,E_F) = \frac{1}{\hbar}\sqrt{\frac{2e^2q|E_F|}{\varepsilon}}. \tag{3}$$

The q dependence of ω_{pl}, namely $\sqrt{q}$, is common to two-dimensional electron gas (2DEG) systems.[11] The existence of plasmons requires that the frequency satisfies

$$\omega_{pl}(q,E_F) > v_F q. \tag{4}$$

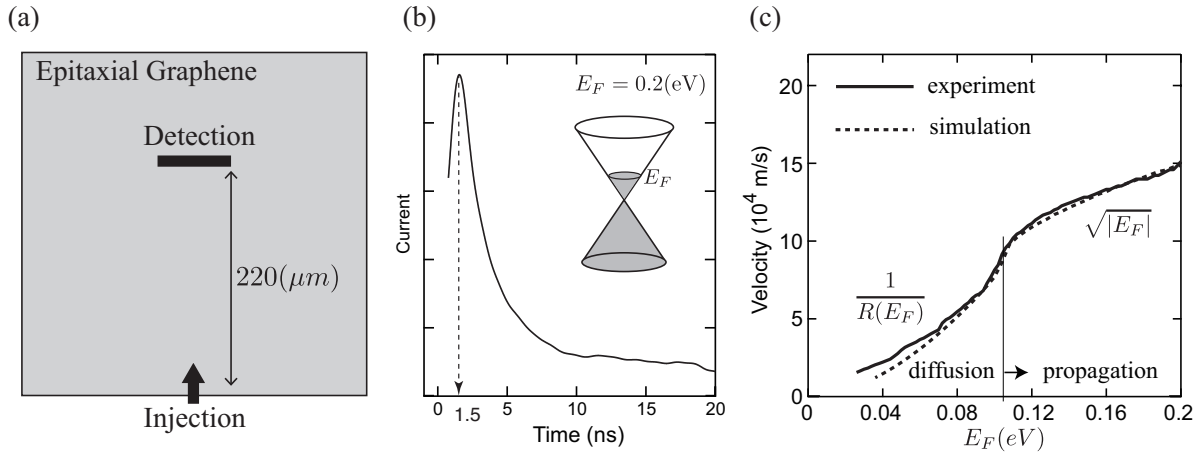

FIG. 1: (a) Schematic of a time-resolved transport experiment on epitaxial graphene.[5] Because the experiments were performed at 1.5 K, the finite temperature effect[7] can be safely ignored. (b) The waveform of the current at the detection gate is given as a function of time. The details of the waveform are dependent on E_F, which is controlled by a metal top gate covering the entire sample. This plot corresponds to $E_F \simeq 0.2$ eV. (c) The E_F dependence of the propagation velocity.

Putting Eq. (3) into this condition, we have

$$\frac{1}{\hbar}\sqrt{\frac{2e^2|E_F|}{\varepsilon q}} > v_F. \tag{5}$$

Because the group velocity is defined by

$$v_g(q, E_F) \equiv \frac{\partial \omega_{pl}(q, E_F)}{\partial q} = \frac{1}{2\hbar}\sqrt{\frac{2e^2|E_F|}{\varepsilon q}}, \tag{6}$$

it is shown that by combining Eq. (5) with Eq. (6) the plasmon group velocity has the lower limit

$$v_g(q, E_F) > \frac{v_F}{2}. \tag{7}$$

This lower limit of the group velocity does not depend on ε, q, E_F, or e^2, whereas the factor $1/2$ reflects the exponent of q in the dispersion relation. The solid line in Fig. 2 shows the lower limit. The actual group velocity must be located above the solid line, as indicated by the vertical arrow. It is also straightforward to show that the group velocity of an undamped plasmon will be located above the dashed curve (see Appendix B for details).

The conditions for the existence of plasmons and for plasmons to be undamped give the lower limit of the propagation velocity, while there is no condition that specifies the upper limit. This result suggests that the propagation velocity of the plasmons is generally high. For example, it is shown by eliminating q from Eq. (6) using Eq. (3) that

$$v_g(\omega_{pl}, E_F) = \frac{e^2}{\hbar\varepsilon}\frac{|E_F|}{\hbar\omega_{pl}}. \tag{8}$$

When $\omega_{pl} = 10$ GHz, $E_F = 0.1$ eV, and $\varepsilon = 10$, we have $v_g \simeq 6 \times 10^7$ m/s.

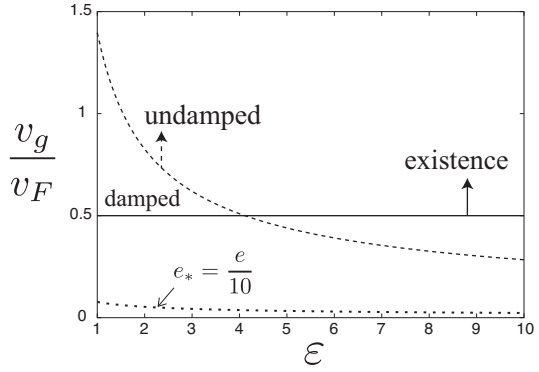

FIG. 2: The lower limit of the group velocity of the plasmons in graphene without a nearby metal top gate. The plasmons cannot exist (are damped) when v_g/v_F is located below the solid line (dashed curve). Screening lowers the dashed curve: the dotted curve is when $e_* = e/10$.

When a metal plate is placed at a distance, d, from a graphene sheet as shown in Fig. 3(a), we have a metal-insulator-graphene device. Nakayama showed that surface plasmons exist for such a device.[12] The dispersion relation is given by

$$\omega_s(q) = \sqrt{\frac{2\pi\sigma_0\tau^{-1}}{\varepsilon}}\sqrt{\frac{q}{1+\coth(qd)}}, \tag{9}$$

where σ_0 is the static conductivity and τ is the relaxation time.[31] In the absence of a metal gate (when $d \to \infty$), we can reproduce Eq. (3) from Eq. (9) using the Einstein relation,[13]

$$\sigma_0 = e^2 v_F^2 \tau D(E_F), \tag{10}$$

where $D(E_F) = 2|E_F|/\pi(\hbar v_F)^2$ is the density of states

of graphene. Thus, Eq. (9) is a general result that includes Eq. (3) as the limiting case. In the presence of a metal gate, the $\sqrt{q}$-dependence is lost for long-wavelength modes (or when $q^{-1} \gg d$) and ω_s exhibits a linear dependence on q as

$$\omega_s(q) = \sqrt{\frac{2\pi\sigma_0\tau^{-1}d}{\varepsilon}}q, \quad (qd \ll 1). \tag{11}$$

Then the group velocity is given by

$$v \equiv \frac{\partial\omega_s(q)}{\partial q} = \sqrt{\frac{2\pi\sigma_0\tau^{-1}d}{\varepsilon}}. \tag{12}$$

The electric fields of surface plasmons have their principal component normal to the graphene sheet $\mathbf{E} = (0, 0, E_z)$, as shown in Fig. 3(a). This field configuration is obtained by solving Maxwell's equations for electromagnetic fields (see Ref. 12 for details). The field configuration is in sharp contrast to that in the absence of a top gate (when $d \to \infty$), where the electric fields have components both normal and parallel to the graphene sheet as $\mathbf{E} = (E_x, 0, E_z)$ where $E_x(x, z, t) = Ee^{i(kx-\omega t)-\alpha|z|}$ and $E_z(x, z, t) = ikE_x(x, z; t)/\alpha$ with $\alpha \equiv \sqrt{k^2 - \varepsilon\omega^2/c^2}$ (see Ref. 12 for details). Because d is 200 nm and the condition $qd \ll 1$ is satisfied in Ref. 5, the excitation described by Eq. (12) is considered to be that observed in the experiment in the presence of a metal top gate. However, the application of the Einstein relation Eq. (10) to Eq. (12) gives

$$v = \frac{e}{\hbar}\sqrt{\frac{4|E_F|d}{\varepsilon}}. \tag{13}$$

The velocity predicted from Eq. (13) with $\varepsilon = 4$ and $d = 200$ nm is $v = 25\sqrt{|E_F|/\mathrm{eV}} \times 10^6$ m/s, which is two orders of magnitude larger than that observed in the experiment (see Fig. 1(c)).

The discrepancy between the predicted and experimental values of velocity can be accounted for by a modification of the Einstein relation caused by a strong (but not perfect) screening effect produced by interface (trap) states. In an epitaxial graphene device grown on SiC, the interface states are naturally realized by the dangling bond states at the SiC substrate [see Fig. 3(b)].[14,15] When the (positive) charge e exists in the graphene sheet, a screening charge with approximately $-e$ is induced on the dangling bond states. Meanwhile, the screening effect of the interface states is not perfect, and a (positive) charge with magnitude e_* remains in the capacitor consisting of the graphene sheet and dangling bond states, as shown schematically in Fig. 3(b).[16] This charge induces (negative) screening charge with $-e_*$ on the metal top gate. If surface plasmons consist of particles with charge magnitude e_*, we can expect Eq. (10) to be defined by replacing e with the screened charge e_* as

$$\sigma_0 = e_*^2 v_{\mathrm{F}}^2 \tau D(E_F). \tag{14}$$

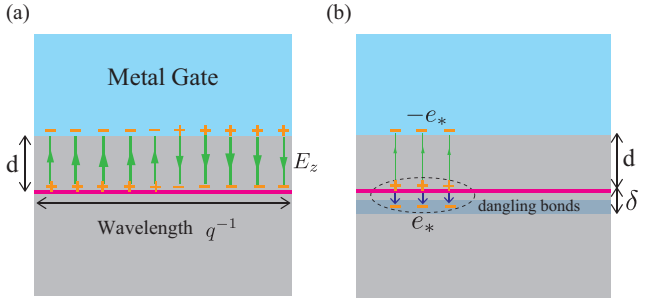

FIG. 3: (color) Cross-section of a device consisting of a graphene sheet (red) and a metal gate (blue). The gray regions represent a dielectric (dielectric constant ε). (a) The arrows represent the electric fields $\mathbf{E} = (0, 0, E_z)$ for non-radiative (acoustic) plasmons satisfying $q^{-1} \gg d$. We omit to draw an exponential decaying electric field which appears underneath the graphene sheet for clarity. (b) Interface states near to graphene sheet, including the dangling bond states ($\delta \ll d$), efficiently screen the electron charge.

The corrected velocity is given by the application of Eq. (14) to Eq. (12) as

$$v = \frac{e_*}{\hbar}\sqrt{\frac{4|E_F|d}{\varepsilon}}. \tag{15}$$

The value of e_* can be roughly estimated by an extension of the result of Luryi,[16] in which e_* is expressed in terms of the quantum capacitance of the interface states C_i [$= e^2\gamma$] and geometrical capacitance C_d [$= \varepsilon/d$] as

$$e_* \simeq \frac{C_d}{C_i + C_d}e, \tag{16}$$

in the static limit. When we adopt the value $\gamma = 0.37$ $\mathrm{eV}^{-1}\cdot\mathrm{nm}^{-2}$ obtained by Takase *et al.*,[15] $e_*/e \simeq 0.036$ for $d = 200$ nm and $\varepsilon = 4$. This value is in agreement with the experiment.[32] The advantage of incorporating screening is that as long as the interface states near to graphene are taken into account through the modification of the Coulomb potential in Eq. (1) as

$$v_q = \frac{2\pi e_*^2}{q}, \tag{17}$$

the conclusion obtained in the absence of a metal top gate is valid even in the presence of the interface states since the lower limit stems from the $\sqrt{q}$-dependence of ω_p and is independent of the electron charge as shown in Eq. (7). This result is also consistent with the experiment.

Propagation velocity can be suppressed by resistivity R, which is not taken into account in Eq. (15). To investigate the effect of R on the propagation velocity, we can adopt an RLC circuit model introduced by Burke *et al.* for studying plasmons in a 2DEG system.[17] The use of this model was motivated by the fact that the electric fields in the dielectric shown in Fig. 3(b) are similar to those in a waveguide, for which the wave propagation is

described by an RLC circuit model. In this model, C and L correspond to C_d and the kinetic inductance of graphene, respectively. In Ref. 5 we simulated the time evolution of the pulse using the Runge-Kutta method and obtained the waveform at the detector. By following the procedure used in the experiment, we determined the propagation velocity of the pulse in terms of the peak time and obtained the dashed curve in Fig. 1(c). Our simulation reproduces the experimental result satisfactorily. The effect of R on the propagation velocity can be examined analytically in terms of the continuum approximation of the RLC circuit model given by the telegrapher's equation,[5,18,19]

$$\left[\frac{\partial^2}{\partial t^2} - v^2\nabla^2 + \frac{R}{L}\frac{\partial}{\partial t}\right] E_z(\mathbf{r},t) = 0, \tag{18}$$

where

$$v = \frac{1}{\sqrt{LC_d}}, \tag{19}$$

and inductance L is given from Eqs. (12) and (14) by

$$L = \frac{\tau}{2\pi\sigma_0} = \frac{1}{2\pi e_*^2 v_F^2 D(E_F)}. \tag{20}$$

The solution may be constructed from the Green's function of the Klein-Gordon equation,

$$\left[\frac{\partial^2}{\partial t^2} - v^2\nabla^2 + m^2\right] \phi(\mathbf{r},t) = 0, \tag{21}$$

with a negative mass squared $m^2 = -q_c^2 v^2$ where q_c is the damping factor,

$$q_c \equiv \frac{R}{2}\sqrt{\frac{C_d}{L}}, \tag{22}$$

because the telegrapher's equation is reproduced from the Klein-Gordon equation by setting $\phi(\mathbf{r},t) = e^{q_c v t} E_z(\mathbf{r},t)$. The retarded Green's function of the Klein-Gordon equation is well-known and written as $\Delta_R(\mathbf{r},t) = \theta(t)\Delta(\mathbf{r},t)$ where

$$\Delta(\mathbf{r},t) = \frac{\mathrm{sgn}(t)}{2\pi}\times \left[\delta(t^2 - \frac{|\mathbf{r}|^2}{v^2}) - \frac{m}{2}\theta(t^2 - \frac{|\mathbf{r}|^2}{v^2})\frac{J_1(m\sqrt{t^2 - \frac{|\mathbf{r}|^2}{v^2}})}{\sqrt{t^2 - \frac{|\mathbf{r}|^2}{v^2}}}\right], \tag{23}$$

and $J_1(x)$ is the Bessel function of the first kind. Thus, by specifying the initial condition $E_z(0,t)$, the solution of the telegrapher's equation is written as $E_z(x,t) = E_p(x,t) + E_d(x,t)$ for $t > x/v$ where[18,19]

$$E_p(x,t) = e^{-q_c x} E_z(0, t - \frac{x}{v}), \tag{24}$$

$$E_d(x,t) = q_c x \int_{\frac{x}{v}}^{t} e^{-q_c v t'} \frac{I_1(q_c v\sqrt{t'^2 - \frac{x^2}{v^2}})}{\sqrt{t'^2 - \frac{x^2}{v^2}}} E_z(0, t - t')dt'. \tag{25}$$

Here, we used $I_1(x) = -iJ_1(ix)$ where $I_1(z)$ is the modified Bessel function of the first kind. Here, $E_p(x,t)$ is an exponentially decaying signal that propagates at a speed v, and $E_d(x,t)$ expresses diffusion.

The effect of R on the plasmon propagation is most clearly visualized at the drop in the peak velocity observed below $E_F \simeq 0.1$ eV in Fig. 1(c) which is due to the dominance of diffusion. For the δ-function initial pulse $E_z(0,t) = \delta(t)$, it is shown that by differentiating Eqs. (24) and (25) with respect to t, the time t^* corresponding to the peak in the waveform is $t^* = x/v$ for $E_p(x,t)$ and $t^* \approx q_c x^2/3v$ for $E_d(x, t \gg x/v)$.[19] Thus, when E_p dominates E_d (propagation dominant), the peak velocity is given by $x/t^* = v$, on the other hand, when E_d dominates E_p (diffusion dominant) the peak velocity is suppressed by the factor of $3/q_c x$ as $x/t^* \approx 3v/q_c x$. Hence, when diffusion dominates, the peak velocity exhibits the E_F dependence of v/q_c ($\propto 1/R$), while when propagation dominates it exhibits the v ($\propto \sqrt{|E_F|}$) dependence. Whether E_d dominates E_p can depend sensitively on the value of q_c. This should be examined for a more realistic initial pulse, namely for the Gaussian initial pulse $E_z(0,t) = \exp(-t^2/T^2)$ where $T = 400$ ps.[5] We plot $E_p(x,t)$, $E_d(x,t)$, and $E_z(x,t)$ at $x = 220$ μm for different q_c values in Fig. 4. When $q_c = 0$, the peak time is seen at $t^* = 2.2$ ns, so the propagation velocity x/t^* is 10^5 m/s, which is approximately equal to the velocity at $E_F = 0.1$ eV in Fig. 1(c). In Fig. 4, it is seen that when $q_c < 0.1$, E_p dominates E_d, whereas when $q_c > 0.3$, E_d dominates E_p. The maximum amplitudes of E_p and E_d are similar when $q_c \simeq 0.2$. The peak time t^* increases rapidly when q_c changes very slightly from 0.2 to 0.3. This means that the peak velocity decreases rapidly then, which can explain that the velocity decreases rapidly below $E_F \simeq 0.1$ eV in Fig. 1(c). Indeed, when we adopt the values obtained in Ref. 5: $R(E_F) = 340 + 3.7\times 10^6/(22 + (500E_F)^2)$ Ω and $\sqrt{C_d/L} = \sqrt{0.58|E_F|}\times 10^{-3}$ Ω^{-1}, q_c changes from 0.218 to 0.283 when E_F decreases a little from 0.1 to 0.08.

Since $E_d(x,t)$ is proportional to q_c, diffusion is suppressed by decreasing q_c, which may be realized by decreasing R or increasing L [see Eq. (22)]. Achieving a large L (or small R) is also important in order to extend the relaxation time $\tau' \equiv 1/(vq_c) = 2L/R$ or to suppress the damping caused by $\exp(-q_c v t)$ for $E_p(x,t)$. However, it should be noted that since both L and R decrease as $|E_F|$ increases, increasing L by decreasing $|E_F|$ is incompatible with decreasing R. On the other hand, L (q_c) is enhanced (suppressed) significantly by the screening effect provided by the interface states.

To conclude, the effects of a metal top gate and interface states on the plasmon transport have been revealed: the former provides linearly dispersed plasmons, while the latter renormalizes the effective charge. In the absence of a metal top gate, the propagation velocity of surface plasmons has a lower limit given by $v_F/2$. This lower limit is a rigid consequence derived from the condition for the existence of plasmons and independent of the electron

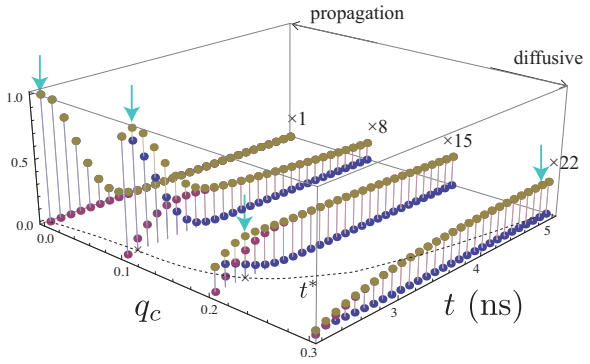

FIG. 4: (color) The q_c-dependence of the waveform at $x = 220$ μm. In this plot we assume $T = 400$ ps and $v = 10^5$ m/s, and q_c is given in the units of $(10\mu m)^{-1}$. The peak time of the E_p component (blue) is $t = 2.2$ ns, while that of the E_d component (red) increases with increasing q_c. The sum of the two components, E_z, is referred by yellow. Arrows represent peak time.

charge in particular. Thus, as long as the interface states are taken into account as the origin of the partial screening effect (i.e., $v_q = 2\pi e^2/q \to 2\pi e_*^2/q$), the conclusion is valid even in the presence of the interface states. In the presence of a metal top gate, the lower limit may be ineffective due to the modification of the dispersion relation of the surface plasmons ($\omega_{pg} \propto \sqrt{q} \to q$). For the linear dispersion, we could utilize the concept of inductance for analyzing the velocity. An analysis using the RLC circuit model and telegrapher's equation successfully explained the experimental results for the E_F dependence of the propagation velocity, which proves that the inductance is effectively enhanced in the presence of a metal top gate. We attributed the enhancement to the screening effect induced by the interface states and found the idea to be consistent with the electron lifetime. A straightforward deduction from our results is that surface plasmons in a device consisting of exfoliated graphene without interface states experiences strong dumping and the propagation is severely suppressed. In other words, epitaxial graphenes have an advantage over exfoliated graphenes in realizing high inductance.

Acknowledgments

We are grateful to Yasuhiro Tokura for helpful discussions.

Appendix A: Polarization function

In this appendix, we use v for v_F and μ for $E_F/\hbar$. The polarization function is given by

$$
\begin{aligned}
&-\mathrm{Im}\Pi_\mu(q,\omega) = \\
&\frac{1}{2\pi}\frac{(vq)^2}{\sqrt{\omega^2-(vq)^2}}\theta_{\omega-vq}\left[\theta_{\frac{\omega-vq}{2}-\mu}\left\{F(1)-F(-1)\right\}+\theta_{\mu-\frac{\omega-vq}{2}}\theta_{\frac{\omega+vq}{2}-\mu}\left\{F(1)-F\left(\frac{2\mu-\omega}{vq}\right)\right\}\right]+ \\
&\frac{1}{2\pi}\frac{(vq)^2}{\sqrt{(vq)^2-\omega^2}}\theta_{vq-\omega}\left[\theta_{\mu-\frac{vq-\omega}{2}}G\left(\frac{2\mu+\omega}{vq}\right)-\theta_{\mu-\frac{\omega+vq}{2}}G\left(\frac{2\mu-\omega}{vq}\right)\right]
\end{aligned}
\tag{A1}
$$

$$
\begin{aligned}
&\mathrm{Re}\Pi_\mu(q,\omega) = -\frac{2\mu}{\pi} \\
&-\frac{1}{2\pi}\frac{(vq)^2}{\sqrt{\omega^2-(vq)^2}}\theta_{\omega-vq}\left[\theta_{\frac{\omega-vq}{2}-\mu}G\left(\frac{\omega-2\mu}{vq}\right)+\theta_{\mu-\frac{\omega+vq}{2}}G\left(\frac{2\mu-\omega}{vq}\right)-G\left(\frac{\omega+2\mu}{vq}\right)\right] \\
&-\frac{1}{2\pi}\frac{(vq)^2}{\sqrt{(vq)^2-\omega^2}}\theta_{vq-\omega}\left[\theta_{\frac{vq+\omega}{2}-\mu}\left\{F(1)-F\left(\frac{2\mu-\omega}{vq}\right)\right\}+\theta_{\frac{vq-\omega}{2}-\mu}\left\{F\left(1\right)-F\left(\frac{\omega+2\mu}{vq}\right)\right\}\right]
\end{aligned}
\tag{A2}
$$

where θ_x denotes the step function satisfying $\theta_{x\geq 0} = 1$ and $\theta_{x<0} = 0$. The functions F and G are defined by

$$F(x) = \frac{1}{2}\left\{x\sqrt{1-x^2}+\sin^{-1}(x)\right\}, \tag{A3}$$

$$G(x) = \frac{1}{2}\left\{x\sqrt{x^2-1}-\ln\left(x+\sqrt{x^2-1}\right)\right\}, \tag{A4}$$

respectively. We showed a direct derivation of the above formula in Supplemental Material of Ref. 10, for which we need to multiply $g_v/(2\pi\hbar v_F)^2$ with $g_v = 2$.

Appendix B

The dashed curve in Fig. 2 is based on the inequality given by

$$v_p(q,E_F) > \frac{e}{2\hbar}\sqrt{\frac{\hbar v_F + \frac{e^2}{2\varepsilon} + \sqrt{\hbar v_F \frac{e^2}{\varepsilon} + \left(\frac{e^2}{2\varepsilon}\right)^2}}{\varepsilon}}. \quad \text{(B1)}$$

This lower limit of the group velocity depends on the values of ε and e. The dotted curve in Fig. 2 is the plot when e is replaced with $e^* = e/10$.

Equation (B1) arises from the fact that plasmons can decay into the constituent (interband) electron-hole pairs of the collective charge-density oscillations. The decay is suppressed (plasmons become undamped) when

$$|E_F| > \frac{\hbar\omega_p(q,E_F) + \hbar v_F q}{2} \quad \text{(B2)}$$

holds, otherwise the decay of plasmons into single particle electron-hole pairs is not negligibly small.[10] Mathematically, Eq. (B2) is equivalent to a condition where the imaginary part of the polarization function Eq. (A1) vanishes: $\mathrm{Im}\Pi_{E_F}(q,\omega_p(q)) = 0$ for $\omega_p(q) > v_F q$. The condition of Eq. (B1) can be obtained by putting Eq. (3) into Eq. (B2) to obtain

$$|E_F| > \frac{q}{2}\left(\hbar v_F + \frac{e^2}{2\varepsilon} + \sqrt{\hbar v_F \frac{e^2}{\varepsilon} + \left(\frac{e^2}{2\varepsilon}\right)^2}\right), \quad \text{(B3)}$$

and then by using Eq. (6).

Appendix C

When $\omega \equiv vq < v_F q$ (or $v < v_F$) and Eq. (B2) is satisfied, the imaginary part of $\Pi_{E_F}(q,\omega)$ is written as

$$-\mathrm{Im}\Pi_{E_F}(q,\omega) = \frac{\hbar v_F q}{4\pi\sqrt{1-\frac{\omega^2}{(v_F q)^2}}} \times \left\{ G\left(\frac{2|E_F| + \hbar\omega}{\hbar v_F q}\right) - G\left(\frac{2|E_F| - \hbar\omega}{\hbar v_F q}\right)\right\}, \quad \text{(C1)}$$

where $G(x) \equiv \left\{x\sqrt{x^2-1} - \log\left(x+\sqrt{x^2-1}\right)\right\}/2$. Note that $dG(x)/dx = \sqrt{x^2-1}$. According to the time-energy uncertainly relation, the mean lifetime is approximated by

$$\tau \equiv -\frac{\hbar}{2\mathrm{Im}\Pi_{E_F}(q,\omega)} \simeq \frac{v_F}{v}\sqrt{1-\left(\frac{v}{v_F}\right)^2}\frac{\pi\hbar}{|E_F|}. \quad \text{(C2)}$$

The characteristic time scale of τ is of the order of a femtosecond because $\tau \simeq 2.5\times 10^{-2}(v_\mathrm{F}/v)|\varepsilon_\mathrm{F}|^{-1}$ fs (ε_F is in units of eV), when $v \ll v_F$.

Appendix D

We examined the d dependence of the electron's quasiparticle lifetime determined by the Coulomb interaction to validate the assumption of screening. The lifetime is given by the inverse of the imaginary part of the electron selfenergy Σ as $\tau_q = \hbar/2\mathrm{Im}\Sigma$. We calculated $\mathrm{Im}\Sigma$ using the formula,[20–22]

$$\mathrm{Im}\Sigma_{\mathbf{k}}(E_F>0) = \int \frac{d^2\mathbf{k}'}{(2\pi)^2}\left\{\theta(\xi_{\mathbf{k}}-\xi_{\mathbf{k}'}) - \theta(\xi_{\mathbf{k}'}-E_F)\right\} \times \frac{1+\cos\left(\Theta_{\mathbf{k}'}-\Theta_{\mathbf{k}}\right)}{2}\mathrm{Im}\frac{v_{|\mathbf{k}'-\mathbf{k}|}}{\varepsilon_{E_F}(|\mathbf{k}'-\mathbf{k}|,\xi_{\mathbf{k}}-\xi_{\mathbf{k}'})}, \quad \text{(D1)}$$

where $\xi_{\mathbf{k}} = \hbar v_F|\mathbf{k}|$, $k_x - ik_y = |\mathbf{k}|\exp(-i\Theta_{\mathbf{k}})$, and v_q denotes the screened Coulomb potential given by

$$v_q = \frac{4\pi e_*^2}{\varepsilon q(1+\coth(qd))}. \quad \text{(D2)}$$

Note that Eq. (15) may be obtained from Eq. (1) with this v_q.[23] A straightforward calculation shows that when $\xi_k \simeq E_F$, $\mathrm{Im}\Sigma_{\mathbf{k}}(E_F>0)$ is approximated by $\hbar v_F|\xi_k - E_F|/(16E_F d)$.[33] As a result, we obtain

$$\tau_q = \frac{8E_F d}{v_F|\xi_k - E_F|}. \quad \text{(D3)}$$

Here let us assume that τ_q is longer than the peak time (t^*). When $|\xi_k - E_F| = 10$ GHz and $d = 200$ nm, τ_q is of the order of ns, which is consistent with the experimental result shown in Fig. 1(b), where the electron peak time is of the order of ns, at least. If $d = 1$ nm, τ_q shortens as $\mathcal{O}$(ps) and is inconsistent with the experiment. Since τ_q is independent of the charge, a unique solution for explaining $v \ll v_F$ is to assume e_* (instead of e) as shown in Eq. (D2) and use Eq. (D2) with Eq. (1).

We note that t^* should not be identified with the transport relaxation time (τ), which is estimated from the mobility μ using $\mu = e_*\tau/m$ where the effective mass m satisfies $mv_F^2/2 = |E_F|$. Because, when $E_F = 0.1$ eV, $\mu \simeq 5000$ cm^2/V·s is the typical value for epitaxial graphene samples,[15] τ is the order of picoseconds. This result is not in good agreement with the experiment showing that t^* is the order of nanoseconds. Even though the Coulomb (electron-electron) interaction provides a finite quasi-particle lifetime, it does not contribute to the transport time. We also note that the plasmon lifetime determined by the Coulomb interaction is estimated in Refs. 24 and 25.

* Electronic address: sasaki.kenichi@lab.ntt.co.jp

[1] G. D. Mahan, *Many-Particle Physics* (Springer, 2000).

[2] T. Ando, Reviews of Modern Physics, **54**, 437 (1982), ISSN 0034-6861.

[3] K. S. Novoselov, A. K. Geim, S. V. Morozov, D. Jiang, M. I. Katsnelson, I. V. Grigorieva, S. V. Dubonos, and A. A. Firsov, Nature, **438**, 197 (2005).

[4] Y. Zhang, Y.-W. Tan, H. L. Stormer, and P. Kim, Nature, **438**, 201 (2005).

[5] N. Kumada, R. Dubourget, K. Sasaki, S. Tanabe, H. Hibino, H. Kamata, M. Hashisaka, K. Muraki, and T. Fujisawa, New Journal of Physics, **16**, 063055 (2014), ISSN 1367-2630.

[6] N. Kumada, S. Tanabe, H. Hibino, H. Kamata, M. Hashisaka, K. Muraki, and T. Fujisawa, Nature communications, **4**, 1363 (2013), ISSN 2041-1723.

[7] G. L. Klimchitskaya, V. M. Mostepanenko, and B. E. Sernelius, Physical Review B, **89**, 125407 (2014), ISSN 1098-0121.

[8] B. Wunsch, T. Stauber, F. Sols, and F. Guinea, New Journal of Physics, **8**, 318 (2006), ISSN 1367-2630.

[9] E. H. Hwang and S. Das Sarma, Physical Review B, **75**, 205418 (2007), ISSN 1098-0121.

[10] K.-i. Sasaki, K. Kato, Y. Tokura, S. Suzuki, and T. Sogawa, Phys. Rev. B, **86**, 201403 (2012).

[11] F. Stern, Physical Review Letters, **18**, 546 (1967), ISSN 0031-9007.

[12] M. Nakayama, J. Phys. Soc. Jpn., **36**, 393 (1974).

[13] T. Ando, Progress of Theoretical Physics Supplement, **176**, 203 (2008), ISSN 0375-9687.

[14] G. Zebrev, in *Physics and Applications of Graphene - Theory*, edited by S. Mikhailov (InTech, 2011) p. 475.

[15] K. Takase, S. Tanabe, S. Sasaki, H. Hibino, and K. Muraki, Phys. Rev. B, **86**, 165435 (2012).

[16] S. Luryi, Applied Physics Letters, **52**, 501 (1988), ISSN 00036951.

[17] P. J. Burke, I. B. Spielman, J. P. Eisenstein, L. N. Pfeiffer, and K. W. West, Appl. Phys. Lett., **76**, 745 (2000).

[18] G. Doetsch, *Guide to the applications of the Laplace and Z-transforms* (Reinhold, 1971).

[19] E. Sonnenschein, I. Rutkevich, and D. Censor, Progress In Electromagnetics Research, **27**, 129 (2000).

[20] J. Quinn and R. Ferrell, Physical Review, **112**, 812 (1958), ISSN 0031-899X.

[21] P. Hawrylak, Physical Review Letters, **59**, 485 (1987), ISSN 0031-9007.

[22] S. Das Sarma, E. Hwang, and W.-K. Tse, Physical Review B, **75**, 121406 (2007), ISSN 1098-0121.

[23] A. Principi, R. Asgari, and M. Polini, Solid State Communications, **151**, 1627 (2011), ISSN 00381098.

[24] A. Principi, G. Vignale, M. Carrega, and M. Polini, Physical Review B, **88**, 121405 (2013), ISSN 1098-0121.

[25] A. Principi, G. Vignale, M. Carrega, and M. Polini, Physical Review B, **88**, 195405 (2013), ISSN 1098-0121.

[26] S. Mikhailov and K. Ziegler, Physical Review Letters, **99**, 016803 (2007), ISSN 0031-9007.

[27] M. Bordag and I. G. Pirozhenko, Physical Review B, **89**, 035421 (2014), ISSN 1098-0121.

[28] P. B. Allen, *From Quantum Mechanics to Technology*, edited by Z. Petru, J. Przystawa, and K. Rapcewicz, Lecture Notes in Physics, Vol. 477 (Springer Berlin Heidelberg, 1997) ISBN 978-3-540-61792-1, pp. 125–141.

[29] We assume that in this paper, the dielectric constant of a metal top gate is $-\infty$ (i.e., a perfect electric conductor for modeling a metal top gate), which is valid at GHz frequencies. The validity of this assumption needs to be checked for frequencies higher than tens of terahertz.

[30] This behavior of $\mathrm{Re}\Pi_{E_F}(q,\omega) < 0$ when $\omega < v_F q$ originates from the fact that softening dominates hardening. Softening/hardening here refers to the negative/positive contributions to the real part of the polarization function. The significance of each contribution depends on the matrix element for the interaction being considered.[10] With the Coulomb interaction, the matrix element is at its maximum (minimum) value for forward (backward) scattering (as shown by $1+\cos(\Theta_{\mathbf{k}'} - \Theta_{\mathbf{k}})$), by which the contribution of the forward (backward) scattering that causes softening (hardening) is enhanced. As a result, softening dominates hardening so that $\mathrm{Re}\Pi_{E_F}(q,\omega) < 0$ when $\omega < v_F q$.

[31] It is assumed that in deriving Eq. (9) the dynamical conductivity σ_ω is approximated by $i\sigma_0/\omega\tau$, which is a direct consequence of the Drude model, $\sigma_\omega = \frac{\sigma_0}{1-i\omega\tau}$, with the condition $\omega\tau \gg 1$. Note that when the imaginary part of the dynamical conductivity is positive as shown above, only a transverse magnetic (TM) mode can exist. Meanwhile when the imaginary part of the dynamical conductivity is negative or in the presence of an external magnetic field, a transverse electric (TE) can appear.[12] Mikhailov and Ziegler point out that the imaginary part of the dynamical conductivity of graphene can be negative for a special frequency,[26] because an interband transition contributes to the dynamical conductivity, while the Drude model only accounts for an intraband transition. As a result, they predict that graphene can support a TE mode for a special frequency (even without an external magnetic field). Another TE mode propagating at the speed of light is reported by Bordag and Pirozhenko,[27] but this can exist only when $E_F = 0$.

[32] Although Eq. (9) is obtained by solving Maxwell's equations for electromagnetic fields in the framework of classical mechanics,[12] when we consider it in quantum mechanics, we can conclude that the frequency does not obey the plasmon existence condition Eq. (4) when $v < v_F$ holds as a result of screening. Indeed, an analysis based on the polarization function suggests that when $v < v_F$, the mean lifetime of the plasmon is of the order of a femtosecond (see Appendix C for details), and the plasmons quickly decay into intraband single-particle electron-hole pairs. In this case, we interpret the plasma surface waves as a density fluctuation consisting of single particle electron-hole pairs.[28] Then it is reasonable to consider that the peak time t^* in the waveform is limited by the quasi-particle lifetime (see Appendix D for details).

[33] The linear dependence of $\mathrm{Im}\Sigma_{\mathbf{k}}$ on $\xi_k - E_F$ is in sharp contrast to the result obtained in the absence of screening,[22] $-\frac{(\xi_k - E_F)^2}{16\pi E_F}\left\{\ln\left(\frac{(\xi_k - E_F)^2}{32E_F^2}\right) + 1\right\}$.